Analytical Method for Vibration of Angle-Ply Cylindrical Shells Having Arbitrary Edges

Y. Narita*

Hokkaido Institute of Technology, Teine Maeda, Sapporo, Japan

and

Y. Ohta,† G. Yamada,‡ and Y. Kobayashi§

Hokkaido University, Kita-ku, Sapporo, Japan

A theoretical method is presented for solving the free vibration of angle-ply laminated cylindrical shells. The angle-ply laminated shell is macroscopically modeled as a thin shell of general anisotropy by using the classical lamination theory. The functional derived from the Flügge-type shell theory is minimized by following the Ritz procedure, and arbitrary combinations of boundary conditions at both ends are accommodated by introducing newly developed admissible functions. A computer code is made to verify the validity of the present method, and the natural frequencies and mode shapes of the laminated cylindrical shells are given for some typical edge conditions numerically.

Introduction

IN recent years, considerable developments have taken place in the structural applications of fiber reinforced composites. Design of lightweight structures often requires a thorough understanding of dynamic behavior of composite components, such as the free vibration frequencies and mode patterns. This need is more obvious when one considers tailoring of composites to meet particular structural requirements.

For the vibrations of laminated cylindrical shells, much work has been done on simply supported cross-ply shells. Dong[1] analyzed vibration of cross-ply laminated shells by using the Donnell-type shell theory, and Dong and Tso[2] considered the effect of shear deformation in the vibration analysis first. Sun and Whitney[3] dealt with axisymmetric vibration of laminated shells, considering normal strains in the thickness direction. Jones and Morgan[4] discussed the influence of the coupling between the inplane and bending motion on vibration and buckling. Uemura[5] used the Novozhilov-type shell theory to discuss the coupling effect for simply supported shells. Sheinman and Greif[6] employed the finite element approach for the simply supported and clamped shells and discussed effects of boundary conditions on the natural frequencies.

Reddy and his co-workers have been quite active in this area. He presented exact solutions, based on the first-order shear deformation theory, for simply supported moderate thick shells.[7] The idea is extended to the higher-order shear deformation theory.[8] Reddy and Khdeir[9] solved the transient response problem to compare the results from various shear deformation theories. They also discussed the effects of the boundary conditions on the natural frequencies.[10] In these papers,[7-10] however, numerical results presented are limited only to the vibration of shallow shell panels, and no results are given for closed cylindrical shells.

Recent literature also includes the work of Kobayashi and Nagashima,[11] which considered nonlinear terms and discussed the influence of the lamination. Sheinman and Weissman[12]

used the finite element method to lead discussions on simplifying Fourier expansions in the circumferential direction for angle-ply shells. Sankaranarayanan et al.[13] considered laminated conical shells of variable thickness in the axial direction. Elishakoff et al.[14] solved the response of thick cross-ply shells subjected to random excitation. All of the previous references, however, presented methods and results for a limited case of boundary conditions, and there is a strong need for straightforward analytical solutions for general boundary conditions, particularly for use of optimization.

The present paper proposes a method to solve the free vibration problem of both angle-ply and cross-ply laminated cylindrical shells, and any combinations of boundary conditions for in-plane and bending motions at both ends are considered. In the analysis, the functional is obtained by using the Flügge-type shell theory, which is well established in vibration analysis, and is minimized with respect to unknown coefficients in the displacement functions. These functions are made to automatically satisfy the geometric boundary conditions (the kinetic boundary conditions) by introducing boundary indices. Based on the method developed, a computer program is made that has input data for the material constants, lamination parameters, and edge conditions (boundary indices). The natural frequencies and mode shapes are presented for various parameters to demonstrate the effectiveness of the present method.

Method of Solution

Figure 1 shows a circular cylindrical shell of the axial length $2L$ and thickness H, and the radius from the center axis to the middle surface is denoted by R. The coordinates (x, θ, z) are taken as in the figure. The shell is laminated with N layers, and the fiber angle in each layer is given by α.
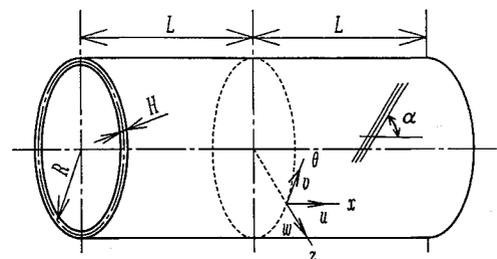
Fig. 1 Angle-ply laminated cylindrical shell and coordinate system.

The stress-strain relation in the kth layer of the shell is given by

$$\begin{Bmatrix} \sigma_x \\ \sigma_\theta \\ \tau_{x\theta} \end{Bmatrix}_{(k)} = \begin{bmatrix} \overline{Q}_{11} & \overline{Q}_{12} & \overline{Q}_{16} \\ \overline{Q}_{12} & \overline{Q}_{22} & \overline{Q}_{26} \\ \overline{Q}_{16} & \overline{Q}_{66} & \overline{Q}_{66} \end{bmatrix}_{(k)} \begin{Bmatrix} \varepsilon_x \\ \varepsilon_\theta \\ \gamma_{x\theta} \end{Bmatrix} \tag{1}$$

where $\sigma_x^{(k)}$, $\sigma_\theta^{(k)}$, $\tau_{x\theta}^{(k)}$, and ε_x, ε_θ, $\gamma_{x\theta}$ are the components of stress and strain, respectively. Material properties of the kth layer are defined by the elastic moduli $\overline{Q}_{ij}^{(k)}$.

The maximum kinetic energy of the shell is expressed as

$$T = \frac{1}{2} \iiint \rho_m \omega^2 [u^2 + v^2 + w^2](R + z)\, dx\, d\theta\, dz \tag{2}$$

in terms of the maximum displacements u, v, and w in the axial, circumferential, and radial directions, respectively, where ρ_m is the mean mass density and ω is the angular frequency. Based on the Flügge-type theory, the maximum strain energy of the shell is expressed as the sum of four parts:

$$U = \frac{1}{2} \iiint [\sigma_x \varepsilon_x + \sigma_\theta \varepsilon_\theta + \tau_{x\theta}\gamma_{x\theta}] (R + z)\, dx\, d\theta\, dz$$

$$= U_{or} + U_{es} + U_{bs} + U_{bt} \tag{3}$$

where U_{or} includes terms that are due to the orthotropic characteristics of material:

$$U_{or} = \frac{R}{2} \iint \left[\overline{A}_{11}\left(\frac{\partial u}{\partial x}\right)^2 + \frac{A_{66}^*}{R^2}\left(\frac{\partial u}{\partial \theta}\right)^2 \right.$$
$$+ \frac{\overline{A}_{22}}{R^2}\left(\frac{\partial v}{\partial \theta}\right)^2 + \left(\overline{A}_{66} + \frac{2\overline{B}_{66}}{R} + \frac{\overline{D}_{66}}{R^2}\right)\left(\frac{\partial v}{\partial x}\right)^2$$
$$+ \frac{A_{22}^*}{R^2} w^2 + \overline{D}_{11}\left(\frac{\partial^2 w}{\partial x^2}\right)^2 + \frac{D_{22}^*}{R^4}\left(\frac{\partial^2 w}{\partial \theta^2}\right)^2$$
$$+ \frac{2D_{12}}{R^2}\frac{\partial^2 w}{\partial x^2}\frac{\partial^2 w}{\partial \theta^2} + \frac{\overline{D}_{66} + 2D_{66} + D_{66}^*}{R^2}\left(\frac{\partial^2 w}{\partial x\partial \theta}\right)^2$$
$$+ \frac{2A_{22}}{R^2}\frac{\partial v}{\partial \theta}w + \frac{2A_{12}}{R}\frac{\partial u}{\partial x}w + \frac{2\overline{A}_{66}}{R}\frac{\partial v}{\partial x}\frac{\partial u}{\partial \theta}$$
$$\left. + \frac{2\overline{A}_{12}}{R}\frac{\partial u}{\partial x}\frac{\partial v}{\partial \theta} \right] dx\, d\theta \tag{4}$$

U_{es} includes terms of extension-shearing coupling:

$$U_{es} = \frac{R}{2} \iint \left[\frac{2A_{16}}{R}\frac{\partial u}{\partial x}\frac{\partial u}{\partial \theta} + \frac{2}{R}\left(\overline{A}_{26} + \frac{\overline{B}_{26}}{R}\right)\frac{\partial v}{\partial x}\frac{\partial v}{\partial \theta} \right.$$
$$+ \frac{2A_{26}}{R^2}\frac{\partial u}{\partial \theta}\frac{\partial v}{\partial \theta} + 2\left(\overline{A}_{16} + \frac{\overline{B}_{16}}{R}\right)\frac{\partial u}{\partial x}\frac{\partial v}{\partial x} + \frac{2\overline{A}_{26}}{R}\frac{\partial v}{\partial x}w$$
$$\left. + \frac{2A_{26}^*}{R^2}\frac{\partial u}{\partial \theta}w \right] dx\, d\theta \tag{5}$$

U_{bs} includes terms of bending-stretching coupling:

$$U_{bs} = -R \iint \left[\frac{B_{22}^*}{R^3}\frac{\partial^2 w}{\partial \theta^2}w + \frac{B_{12}}{R}\frac{\partial^2 w}{\partial x^2}w \right.$$
$$+ \frac{B_{26} + B_{26}^*}{R^2}\frac{\partial^2 w}{\partial x\partial \theta}w + \left(\overline{B}_{16} + \frac{\overline{D}_{16}}{R}\right)\frac{\partial v}{\partial x}\frac{\partial^2 w}{\partial x^2}$$
$$+ \frac{\overline{B}_{26} + B_{26}}{R^2}\frac{\partial v}{\partial \theta}\frac{\partial^2 w}{\partial x\partial \theta} + \frac{1}{R^2}\left(B_{26} + \frac{D_{26}}{R}\right)\frac{\partial v}{\partial x}\frac{\partial^2 w}{\partial \theta^2}$$
$$+ \frac{\overline{B}_{12}}{R}\frac{\partial v}{\partial \theta}\frac{\partial^2 w}{\partial x^2} + \frac{1}{R}\left(2\overline{B}_{66} + \frac{\overline{D}_{66}}{R}\right)\frac{\partial v}{\partial x}\frac{\partial^2 w}{\partial x\partial \theta} + \frac{B_{22}}{R^3}\frac{\partial v}{\partial \theta}\frac{\partial^2 w}{\partial \theta^2}$$

$$+ \overline{B}_{11}\frac{\partial u}{\partial x}\frac{\partial^2 w}{\partial x^2} + \frac{B_{66} + B_{66}^*}{R^2}\frac{\partial u}{\partial \theta}\frac{\partial^2 w}{\partial x\partial \theta} + \frac{B_{12}}{R^2}\frac{\partial u}{\partial x}\frac{\partial^2 w}{\partial \theta^2}$$
$$+ \frac{B_{16}}{R}\frac{\partial u}{\partial \theta}\frac{\partial^2 w}{\partial x^2} + \frac{\overline{B}_{16} + B_{16}}{R}\frac{\partial u}{\partial x}\frac{\partial^2 w}{\partial x\partial \theta}$$
$$+ \frac{B_{26}^*}{R^3}\frac{\partial u}{\partial \theta}\frac{\partial^2 w}{\partial \theta^2} \Bigg] dx\, d\theta \tag{6}$$

and U_{bt} includes terms of bending-twisting coupling:

$$U_{bt} = R \iint \left[\frac{\overline{D}_{16} + D_{16}}{R}\frac{\partial^2 w}{\partial x^2}\frac{\partial^2 w}{\partial x\partial \theta} \right.$$
$$\left. + \frac{D_{26} + D_{26}^*}{R^3}\frac{\partial^2 w}{\partial \theta^2}\frac{\partial^2 w}{\partial x\partial \theta} \right] dx\, d\theta \tag{7}$$

with $\overline{A}_{ij}$, $\overline{B}_{ij}$, $\overline{D}_{ij}$, A_{ij}, B_{ij}, D_{ij}, A_{ij}^*, B_{ij}^*, and D_{ij}^* being the stiffness coefficients defined as

$$\overline{A}_{ij} = A_{ij} + \frac{B_{ij}}{R}, \quad \overline{B}_{ij} = B_{ij} + \frac{D_{ij}}{R}, \quad \overline{D}_{ij} = D_{ij} + \frac{E_{ij}}{R} \tag{8a}$$

$$(A_{ij}, B_{ij}, D_{ij}, E_{ij}) = \sum_{k=1}^{N} \int_z \overline{Q}_{ij}^{(k)} (1, z, z^2, z^3)\, dz \tag{8b}$$

$$(A_{ij}^*, B_{ij}^*, D_{ij}^*) = \sum_{k=1}^{N} \int_z \overline{Q}_{ij}^{(k)} \left(1 + \frac{z}{R}\right)^{-1} (1, z, z^2)\, dz \tag{8c}$$

For simplicity of the analysis, the following dimensionless quantities are introduced:

$$\xi = x/L, \quad \eta = z/H, \quad (l, h) = (1/R)(L, H) \tag{9a}$$

$$(\bar{u}, \bar{v}, \bar{w}) = (1/H)(u, v, w), \quad \lambda^2 = \rho_0 R^2 \omega^2 / E_0 \tag{9b}$$

$$(\bar{a}_{ij}, a_{ij}, a_{ij}^*) = (1/E_0 R)(\overline{A}_{ij}, A_{ij}, A_{ij}^*) \tag{9c}$$

$$(\bar{b}_{ij}, b_{ij}, b_{ij}^*) = (1/E_0 R^2)(\overline{B}_{ij}, B_{ij}, B_{ij}^*) \tag{9d}$$

$$(\bar{d}_{ij}, d_{ij}, d_{ij}^*) = (1/E_0 R^3)(\overline{D}_{ij}, D_{ij}, D_{ij}^*) \tag{9e}$$

where ρ_0 and E_0 are the representative mass density and Young's modulus, respectively, and λ is a nondimensional frequency parameter.

The displacements of the shell are expressed as

$$\bar{u}(\xi, \theta) = \sum_{i=1}^{I} \sum_{j=1}^{J} U_{ij} X_{1i} Y_j(\theta)$$

$$= \sum_{i=1}^{I} \sum_{j=1}^{J} U_{ij} \xi^{i-1}(1 + \xi)^{\alpha_1}(1 - \xi)^{\beta_1} Y_j(\theta) \tag{10a}$$

$$\bar{v}(\xi, \theta) = \sum_{i=1}^{I} \sum_{j=1}^{J} V_{ij} X_{2i} Y_j(\theta)$$

$$= \sum_{i=1}^{I} \sum_{j=1}^{J} V_{ij} \xi^{i-1}(1 + \xi)^{\alpha_2}(1 - \xi)^{\beta_2} Y_j(\theta) \tag{10b}$$

$$\bar{w}(\xi, \theta) = \sum_{i=1}^{I} \sum_{j=1}^{J} W_{ij} X_{3i} Y_j(\theta)$$

$$= \sum_{i=1}^{I} \sum_{j=1}^{J} W_{ij} \xi^{i-1}(1 + \xi)^{\alpha_3}(1 - \xi)^{\beta_3} Y_j(\theta) \tag{10c}$$

with

$$Y_j(\theta) = \cos\{(j - 1)\theta/2\} \quad (j : \text{odd})$$
$$= \sin\{j\,\theta/2\} \quad (j : \text{even}) \tag{10d}$$

where α_i and β_i ($i = 1, 2, 3$) are boundary indices introduced such that the displacement functions (10) automatically satisfy given geometric boundary conditions. For example, at the left-hand edge ($x = -L$), $\alpha_1 = 0$ denotes the in-plane movable edge and $\alpha_1 = 1$ denotes the immovable edge in the axial direction; α_2 is similarly defined in the circumferential direction. For the out-of-plane motion, $\alpha_3 = 0$ denotes no constraints, $\alpha_3 = 1$ denotes that only transverse motion is constrained (i.e., no constraint on rotation), and $\alpha_3 = 2$ denotes the clamped edge.

For the typical edge conditions:

$$\alpha_1 = \beta_1 = 0, \quad \alpha_2 = \beta_2 = \alpha_3 = \beta_3 = 1$$

for a simply supported-simply supported shell,

$$\alpha_1 = \beta_1 = \alpha_2 = \beta_2 = 1, \quad \alpha_3 = \beta_3 = 2$$

for a clamped-clamped shell, and

$$\alpha_1 = \alpha_2 = 1, \quad \alpha_3 = 2, \quad \beta_1 = \beta_2 = \beta_3 = 0$$

for a clamped-free shell.

By substituting Eqs. (10) into Eqs. (2) and (3), and minimizing the Lagrange functional $L = T - U$ for a stationary value, the following frequency equation is derived:

$$\begin{bmatrix} K_{ij}^{(mn)} - \lambda^2 X_{ij}^{(mn)} & & \text{sym.} \\ N_{ij}^{(mn)} & L_{ij}^{(mn)} - \lambda^2 Y_{ij}^{(mn)} & \\ O_{ij}^{(mn)} & P_{ij}^{(mn)} & M_{ij}^{(mn)} - \lambda^2 Z_{ij}^{(mn)} \end{bmatrix} \begin{Bmatrix} U_{ij} \\ V_{ij} \\ W_{ij} \end{Bmatrix} = 0$$

$$(i, m = 1, 2, \ldots, I; j, n = 1, 2, \ldots, J) \quad (11)$$

The elements of Eq. (11) are given by

$$K_{ij}^{(mn)} = \frac{\bar{a}_{11}}{l^2} f_{11mi}^{11} g_{nj}^{00} + a_{66}^* f_{11mi}^{00} g_{nj}^{11}$$

$$+ \frac{a_{16}}{l} (f_{11mi}^{10} g_{nj}^{01} + f_{11mi}^{01} g_{nj}^{10}) \quad (12a)$$

$$L_{ij}^{(mn)} = \bar{a}_{22} f_{22mi}^{00} g_{nj}^{11} + \frac{\bar{a}_{66} + 2\bar{b}_{66} + \bar{d}_{66}}{l^2} f_{22mi}^{11} g_{nj}^{00}$$

$$+ \frac{\bar{a}_{26} + \bar{b}_{26}}{l} (f_{22mi}^{10} g_{nj}^{01} + f_{22mi}^{01} g_{nj}^{10}) \quad (12b)$$

$$M_{ij}^{(mn)} = a_{22}^* f_{33mi}^{00} g_{nj}^{00} + \frac{\bar{d}_{11}}{l^4} f_{33mi}^{22} g_{nj}^{00} + d_{22}^* f_{33mi}^{00} g_{nj}^{22}$$

$$+ \frac{d_{12}}{l^2} (f_{33mi}^{20} g_{nj}^{02} + f_{33mi}^{02} g_{nj}^{20})$$

$$+ \frac{\bar{d}_{66} + 2d_{66} + d_{66}^*}{l^2} f_{33mi}^{11} g_{nj}^{11}$$

$$- b_{22}^* (f_{33mi}^{00} g_{nj}^{02} + f_{33mi}^{00} g_{nj}^{20})$$

$$- \frac{b_{12}}{l^2} (f_{33mi}^{02} g_{nj}^{00} + f_{33mi}^{20} g_{nj}^{00})$$

$$- \frac{b_{26} + b_{26}^*}{l} (f_{33mi}^{01} g_{nj}^{01} + f_{33mi}^{10} g_{nj}^{10})$$

$$+ \frac{\bar{d}_{16} + d_{16}}{l^3} (f_{33mi}^{21} g_{nj}^{01} + f_{33mi}^{12} g_{nj}^{10})$$

$$+ \frac{d_{26} + d_{26}^*}{l} (f_{33mi}^{01} g_{nj}^{21} + f_{33mi}^{10} g_{nj}^{12}) \quad (12c)$$

$$N_{ij}^{(mn)} = \frac{\bar{a}_{66}}{l} f_{21mi}^{10} g_{nj}^{01} + \frac{\bar{a}_{12}}{l} f_{21mi}^{01} g_{nj}^{10} + \frac{\bar{a}_{16}}{l^2} f_{21mi}^{11} g_{nj}^{00}$$

$$+ a_{26} f_{21mi}^{00} g_{nj}^{11} + \frac{\bar{b}_{16}}{l^2} f_{21mi}^{11} g_{nj}^{00} \quad (12d)$$

$$O_{ij}^{(mn)} = \frac{a_{12}}{l} f_{31mi}^{01} g_{nj}^{00} + a_{26}^* f_{31mi}^{00} g_{nj}^{01} - \frac{\bar{b}_{11}}{l^3} f_{31mi}^{21} g_{nj}^{00}$$

$$- \frac{b_{66} + b_{66}^*}{l} f_{31mi}^{10} g_{nj}^{11} - \frac{b_{12}}{l} f_{31mi}^{01} g_{nj}^{20} - \frac{b_{16}}{l^2} f_{31mi}^{20} g_{nj}^{01}$$

$$- \frac{\bar{b}_{16} + b_{16}}{l^2} f_{31mi}^{11} g_{nj}^{10} - b_{26}^* f_{31mi}^{00} g_{nj}^{21} \quad (12e)$$

$$P_{ij}^{(mn)} = a_{22} f_{32mi}^{00} g_{nj}^{01} - \frac{\bar{b}_{16}}{l^3} f_{32mi}^{21} g_{nj}^{00} - \frac{\bar{b}_{26} + b_{26}}{l} f_{32mi}^{10} g_{nj}^{11}$$

$$- \frac{b_{26}}{l} f_{32mi}^{01} g_{nj}^{20} - \frac{b_{12}}{l^2} f_{32mi}^{20} g_{nj}^{01} - \frac{2\bar{b}_{66} + \bar{d}_{66}}{l^2} f_{32mi}^{11} g_{nj}^{10}$$

$$- b_{22} f_{32mi}^{00} g_{nj}^{21} + \frac{\bar{a}_{26}}{l} f_{32mi}^{01} g_{nj}^{00} - \frac{\bar{d}_{16}}{l^3} f_{32mi}^{21} g_{nj}^{00}$$

$$- \frac{d_{26}}{l} f_{32mi}^{01} g_{nj}^{20} \quad (12f)$$

$$X_{ij}^{(mn)} = \bar{I} f_{11mi}^{00} g_{nj}^{00}, \quad Y_{ij}^{(mn)} = \bar{I} f_{22mi}^{00} g_{nj}^{00}$$

$$Z_{ij}^{(mn)} = \bar{I} f_{33mi}^{00} g_{nj}^{00} \quad (12g)$$

$$\bar{I} = \sum_{k=1}^{N} \int \frac{\rho^{(k)}}{\rho_0} h(1 + h\eta) \, d\eta \quad (12h)$$

where $\rho^{(k)}$ is the mass density of the kth layer of the shell, and f_{klmn}^{ij} and g_{mn}^{ij} are integrals defined by

$$f_{klmn}^{ij} = \int_{-1}^{1} \frac{\partial^{(i)} X_{km}}{\partial \xi^{(i)}} \frac{\partial^{(j)} X_{ln}}{\partial \xi^{(j)}} \, d\xi \quad (13a)$$

$$g_{mn}^{ij} = \int_{0}^{2\pi} \frac{\partial^{(i)} Y_m}{\partial \theta^{(i)}} \frac{\partial^{(j)} Y_n}{\partial \theta^{(j)}} \, d\theta \quad (13b)$$

The determinant of the coefficient matrix of Eq. (11) is set equal to zero, which yields eigenvalues (frequency parameters), and substituting each eigenvalue back into Eq. (11) gives the corresponding eigenvector (amplitude ratio) in the usual manner.

Numerical Results and Discussions

By using the scheme described in the previous section, a numerical study is carried out for cylindrical shells having small thickness ratio ($h = 0.01$) and moderate length ($l = 2$). A graphite/epoxy, which is a highly orthotropic fiber-reinforced material, is selected, and the material properties used are $E_1/E_2 = 20$, $G_{12}/E_2 = 0.65$, and $\nu_{12} = 0.25$ (subscript 1 denotes the major material-symmetry direction, and subscript 2 denotes the in-plane transverse direction). The layer sequence is described by using subscripts S and A for symmetric and antisymmetric lamination, respectively; for instance, $[\alpha, -\alpha]_s$ denotes a four-layered shell with the symmetric fiber sequence $[\alpha, -\alpha, -\alpha, \alpha]$ from inner to outer of the shell, and E_2 is used as the base modulus in frequency parameters λ.

Convergence and Comparison

Accuracy of numerical results depends on the number of terms I, J used in the displacement functions (10), and convergence studies are made in Table 1 for the lowest five frequencies of the shells with [45 deg, -45 deg]$_s$ and [45 deg,

Table 1 Convergence characteristics of frequency parameters λ of angle-ply laminated cylindrical shells
($l = 2.0$, $h = 0.01$, $E_1 = 20E_2$, $G_{12} = 0.65E_2$, $\nu_{12} = 0.25$)

Boundary conditions	Lamination, deg	$I \times J$	First	Second	Third	Fourth	Fifth
SS	$[45, -45]_s$	5×11	0.1194	0.1254	0.1736	0.2204	0.2591
		6×13	0.1193	0.1254	0.1734	0.2203	0.2364
		7×15	0.1193	0.1254	0.1734	0.2203	0.2362
		8×17	0.1193	0.1253	0.1733	0.2203	0.2362
	$[45, -45]_A$	5×11	0.1171	0.1195	0.1683	0.2202	0.2446
		6×13	0.1171	0.1195	0.1683	0.2201	0.2382
		7×15	0.1171	0.1195	0.1683	0.2201	0.2382
		8×17	0.1171	0.1195	0.1683	0.2201	0.2382
CC	$[45, -45]_s$	5×11	0.1838	0.1976	0.2541	0.3422	0.4372
		6×13	0.1824	0.1965	0.2484	0.2522	0.3315
		7×15	0.1791	0.1955	0.2446	0.2479	0.3171
		8×17	0.1789	0.1951	0.2444	0.2474	0.3168
	$[45, -45]_A$	5×11	0.1793	0.1911	0.2530	0.3321	0.4338
		6×13	0.1779	0.1902	0.2475	0.2510	0.3217
		7×15	0.1745	0.1889	0.2434	0.2470	0.3205
		8×17	0.1744	0.1888	0.2432	0.2469	0.3159
CF	$[45, -45]_s$	5×11	0.0677	0.0828	0.1039	0.1550	0.1902
		6×13	0.0674	0.0813	0.1036	0.1545	0.1875
		7×15	0.0667	0.0800	0.1032	0.1543	0.1863
		8×17	0.0665	0.0793	0.1027	0.1536	0.1847
	$[45, -45]_A$	5×11	0.0648	0.0825	0.1008	0.1581	0.1830
		6×13	0.0645	0.0810	0.1007	0.1580	0.1803
		7×15	0.0639	0.0796	0.1003	0.1576	0.1794
		8×17	0.0638	0.0789	0.1002	0.1573	0.1778

-45 deg$]_A$ lamination. Three types of edge conditions are considered: 1) both edges simply supported (SS), 2) both edges clamped (CC), 3) and cantilever support (CF). The boundary conditions for simply supported edges are $u \neq 0$, $v = 0$, $w = 0$, and $\partial w/\partial x \neq 0$, and those for clamped and free edges imply that motions are totally constrained ($u = v = w = \partial w/\partial x = 0$) and unconstrained ($u \neq 0$, $v \neq 0$, $w \neq 0$, $\partial w/\partial x \neq 0$), respectively. In Table 1, the SS shell yields fast convergence speed and most of frequency values are converged within four significant figures. The other two shells (CC, CF) show relatively slow convergence. On the whole, however, the present method gives accurate upper bounds when enough terms are used for both axial and circumferential directions. Based on the convergence test, the following calculations are made by using $I \times J = 8 \times 17$ terms.

Comparison with other results is also made in Table 2 to establish the accuracy of the present method. Kobayashi and Nagashima[11] obtained results for cross-ply laminated SS and CC shells ($h = 0.0025$, $l = 1$) with two and four layers. The

Table 2 Comparison of frequency parameters λ of cross-ply laminated cylindrical shells ($l = 1.0$, $h = 0.0025$, $E_1 = 15.59E_2$, $G_{12} = 0.5366E_2$, $\nu_{12} = 0.32$, $I \times J = 8 \times 17$)

Boundary conditions	Lamination,[a] deg	Present	Ref. 11
SS	$[90, 0]$	0.1246	0.1245
	$[0, 90]$	0.1200	0.1200
	$[0, 90]_A$	0.1412	0.1412
	$[90, 0]_A$	0.1431	0.1430
	$[0, 90]_s$	0.1170	0.1170
	$[90, 0]_s$	0.1649	0.1648
CC	$[90, 0]$	0.1535	0.1526
	$[0, 90]$	0.1517	0.1509

[a][inner, outer]

material constants in this case are $E_1/E_2 = 15.59$, $G_{12}/E_2 = 0.5366$, and $\nu_{12} = 0.32$. Most of their results for the SS shell agree with the present ones with four significant figures. For the CC shell, discrepancies are only 0.5%. The comparison thus shows the validity of the present method.

a) SS-SS shell

b) C-C shell

c) C-F shell
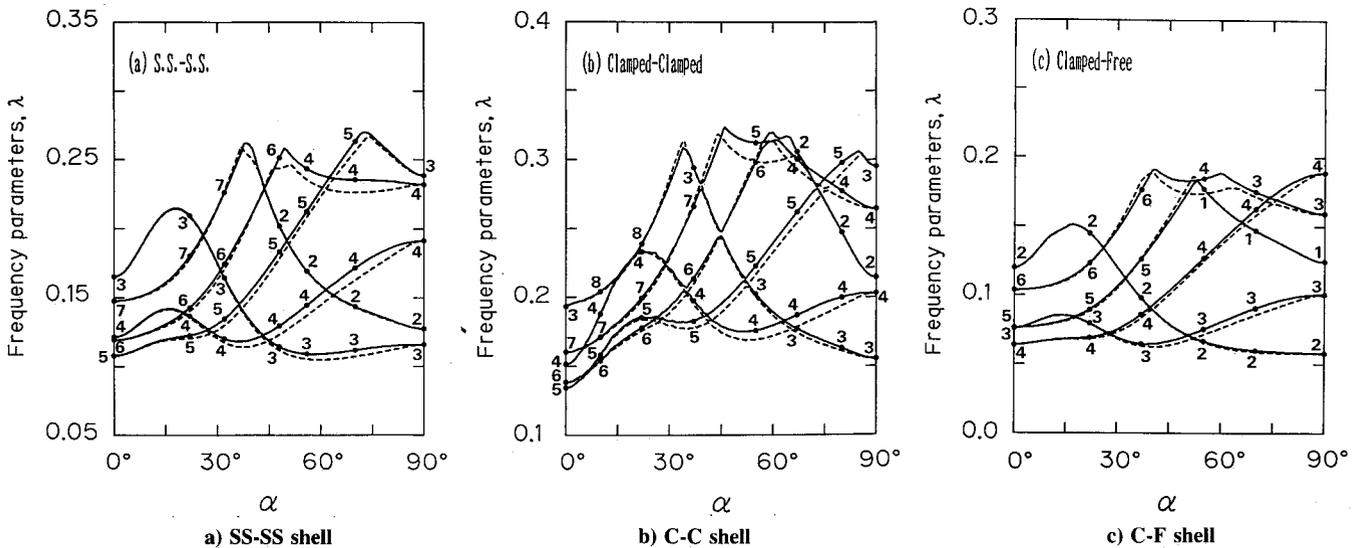
Fig. 2 Frequency variation λ of angle-ply cylindrical shells with fiber angle α : $l = 2.0$, $h = 0.01$, $E_1/E_2 = 20$, $G_{12}/E_2 = 0.65$, $\nu_{12} = 0.25$.

Table 3 Frequency parameters λ of angle-ply laminated cylindrical shells
$(l = 2.0, h = 0.01, E_1 = 20E_2, G_{12} = 0.65E_2, \nu_{12} = 0.25, I \times J = 8 \times 17)$

Boundary conditions	Lamination, deg	First	Second	Third	Fourth	Fifth
SS	$[30, -30]_s$	0.1232	0.1314	0.1675	0.1753	0.2160
	$[30, -30]_A$	0.1209	0.1273	0.1640	0.1746	0.2161
	$[45, -45]_s$	0.1193	0.1253	0.1733	0.2203	0.2362
	$[45, -45]_A$	0.1171	0.1195	0.1683	0.2201	0.2382
	$[60, -60]_s$	0.1093	0.1533	0.1597	0.2283	0.2392
	$[60, -60]_A$	0.1052	0.1454	0.1592	0.2238	0.2305
CC	$[30, -30]_s$	0.1827	0.1925	0.2212	0.2295	0.2811
	$[30, -30]_A$	0.1793	0.1884	0.2196	0.2281	0.2855
	$[45, -45]_s$	0.1789	0.1951	0.2444	0.2474	0.3168
	$[45, -45]_A$	0.1744	0.1888	0.2432	0.2469	0.3159
	$[60, -60]_s$	0.1796	0.1894	0.2391	0.3136	0.3196
	$[60, -60]_A$	0.1721	0.1870	0.2325	0.2984	0.3130
CF	$[30, -30]_s$	0.0694	0.0750	0.1059	0.1204	0.1470
	$[30, -30]_A$	0.0686	0.0731	0.1047	0.1203	0.1494
	$[45, -45]_s$	0.0665	0.0793	0.1027	0.1536	0.1847
	$[45, -45]_A$	0.0638	0.0789	0.1002	0.1573	0.1778
	$[60, -60]_s$	0.0633	0.0806	0.1390	0.1641	0.1880
	$[60, -60]_A$	0.0624	0.0762	0.1363	0.1641	0.1758

Table 4 Geometric boundary conditions of angle-ply laminated cylindrical shells

Notation	Geometric boundary conditions at both edges			
1	$u \neq 0,$	$v \neq 0,$	$w \neq 0,$	$\dfrac{\partial w}{\partial x} \neq 0$
2	$u = 0,$	$v \neq 0,$	$w \neq 0,$	$\dfrac{\partial w}{\partial x} \neq 0$
3	$u \neq 0,$	$v = 0,$	$w \neq 0,$	$\dfrac{\partial w}{\partial x} \neq 0$
4	$u \neq 0,$	$v \neq 0,$	$w = 0,$	$\dfrac{\partial w}{\partial x} \neq 0$
5	$u \neq 0,$	$v \neq 0,$	$w = 0,$	$\dfrac{\partial w}{\partial x} = 0$
6	$u = 0,$	$v = 0,$	$w \neq 0,$	$\dfrac{\partial w}{\partial x} \neq 0$
7	$u = 0,$	$v \neq 0,$	$w = 0,$	$\dfrac{\partial w}{\partial x} \neq 0$
8	$u \neq 0,$	$v = 0,$	$w = 0,$	$\dfrac{\partial w}{\partial x} \neq 0$
9	$u = 0,$	$v \neq 0,$	$w = 0,$	$\dfrac{\partial w}{\partial x} = 0$
10	$u \neq 0,$	$v = 0,$	$w = 0,$	$\dfrac{\partial w}{\partial x} = 0$
11	$u = 0,$	$v = 0,$	$w = 0,$	$\dfrac{\partial w}{\partial x} \neq 0$
12	$u = 0,$	$v = 0,$	$w = 0,$	$\dfrac{\partial w}{\partial x} = 0$

Table 5 Frequency parameters λ of angle-ply laminated cylindrical shells $(l = 2.0, h = 0.01, E_1 = 20E_2, G_{12} = 0.65E_2, \nu_{12} = 0.25,$ [45 deg, -45 deg]$_s$, $I \times J = 8 \times 17)$

| Boundary conditions	First	Second	Third	Fourth	Fifth
1	0.0160[2]	0.0259[2]	0.0469[3]	0.0651[3]	0.0905[4]
2	0.0190[2]	0.0532[3]	0.0985[4]	0.1193[3]	0.1274[4]
3	0.1193[3]	0.1252[4]	0.1732[5]	0.2203[2]	0.2359[6]
4	0.1147[3]	0.1244[4]	0.1720[2]	0.1725[5]	0.1892[1]
5	0.1239[3]	0.1288[4]	0.1754[5]	0.2045[2]	0.2378[6]
6	0.1694[4]	0.1905[5]	0.2260[3]	0.2445[6]	0.3089[5]
7	0.1713[4]	0.1830[1]	0.1921[5]	0.2059[3]	0.2331[2]
8	0.1193[3]	0.1253[4]	0.1733[5]	0.2203[2]	0.2362[6]
9	0.1781[4]	0.1941[5]	0.2432[3]	0.2469[6]	0.3066[1]
10	0.1240[3]	0.1302[4]	0.1769[5]	0.2224[2]	0.2387[6]
11	0.1733[4]	0.1925[5]	0.2331[3]	0.2459[6]	0.3157[7]
12	0.1789[4]	0.1951[5]	0.2444[3]	0.2474[6]	0.3168[7]

Frequencies for Angle-Ply Laminated Cylindrical Shells

Figures 2a–2c present variations in frequency parameter λ with the angle α for SS, CC, and CF cylindrical shells, respectively. The shells have the symmetric four-layer sequence $[\alpha, -\alpha]_s$ (shown by solid lines in the figures) and the antisymmetric sequence $[\alpha, -\alpha]_A$ (shown by broken lines). The frequency variations are depicted by fitting smooth curves to calculated results. When two frequencies approach each other as α is changed, behaviors of these curves are closely examined. In some cases, the curves veer away, whereas in the other cases, the curves appear to cross. The integer given at a dot in the figure denotes the dominant circumferential wave number for out-of-plane displacement w, which is detected by drawing a nodal pattern of each mode for particular α.

The frequencies for the three shells (SS, CC, CF) vary considerably with the fiber angle α. These variations occur mainly because the principal material axes are skewed with the angle-ply stacking sequence. The geometric parameters and boundary conditions of the shell also have effects on the variations. For the fundamental (lowest) mode, the wave number varies $5\rightarrow4\rightarrow3$ for the SS shell, $5\rightarrow6\rightarrow5\rightarrow4\rightarrow3$ for the CC shell, and $4\rightarrow3\rightarrow2$ for the CF shell, as the angle α is increased from 0 to 90 deg. Thus, the circumferential wave number gradually decreases with α because the shell is stiffened more in the circumferential direction by the fibers with increasing α. Among the three shells, the CF shell shows relatively lower wave numbers and the third mode for $\alpha >$ 65 deg has only one wave.

The frequency parameters λ used in Figs. 2 are listed in Table 3 for $\alpha = 30, 45,$ and 60 deg. It is seen that the symmetrically laminated shells yield greater values than the antisymmetrically laminated shells, except for some case in the fourth and fifth modes.

The present method can accommodate any combinations of boundary conditions for in-plane and out-of-plane motions,
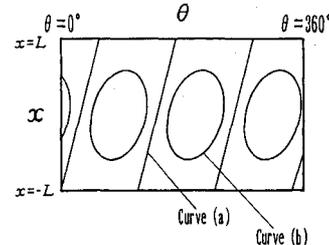
Fig. 3 Mode pattern representation for developed shell surface.

and as previously mentioned, the conditions for both edges can be selected as input data in the computer code. To demonstrate the effectiveness of this method, frequency parameters for the shell with various edge conditions are calculated. There exist 12 possible cases at one end because there are two choices (free or constrained) for two in-plane motions u, v and three choices (free, supported, or clamped) for the out-of-plane motion w. The shell has more cases when one considers combinations at both ends.

Table 4 shows the 12 combinations of boundary conditions, wherein case 1 is a totally free shell and case 12 is a totally constrained shell. Cases 2–4 have only one constraint among a possible of four constraints, cases 5–8 have two constraints, and cases 9–11 have three constraints. Therefore, the cases between the two extreme cases are given in order somehow to reflect gradual increase of constraints. Table 5 presents the lowest five frequencies for the shell with the boundary conditions listed in Table 4. Both edges are assumed to have the same conditions to limit the number of combinations. The integer given at the upper right for each frequency is the circumferential wave number. Generally speaking, the wave number for the lowest mode increases as more constraints are added to both edges.

Mode Shapes for Angle-Ply Laminated Cylindrical Shells

The mode shapes of the out-of-plane displacement w for the four-layered cylindrical shells are presented in this section. Figure 3 shows an example of the mode pattern representation, where a developed surface of a closed cylindrical shell is given. Typically, skewed lines from one end to the other (curve a) are nodal lines (i.e., lines of zero deflection) and oval lines (curve b) denote contour lines representing half of the maximum deflection.
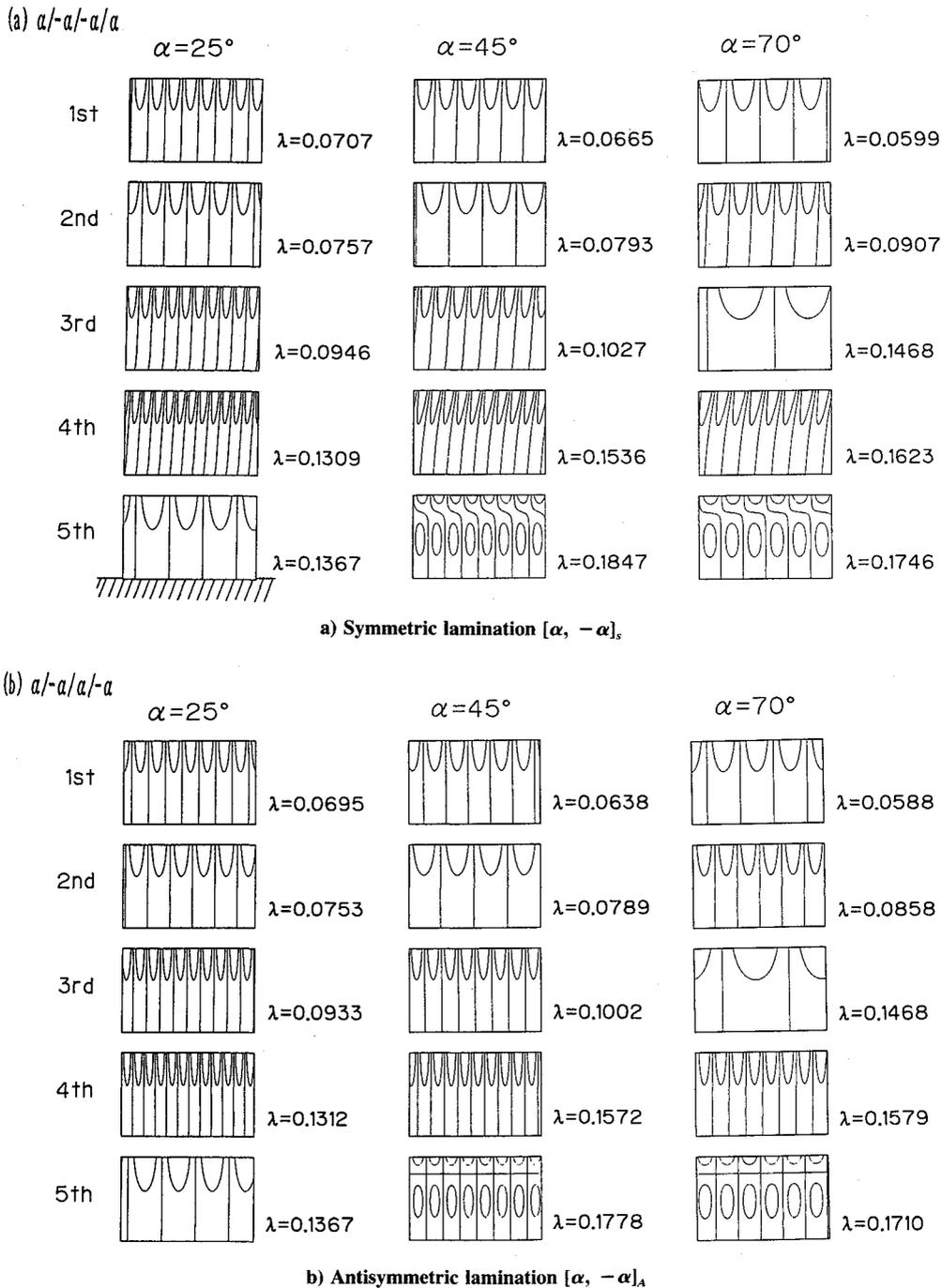

a) Symmetric lamination $[\alpha, -\alpha]_s$

b) Antisymmetric lamination $[\alpha, -\alpha]_A$

Fig. 4 Mode shapes of four-layered cylindrical shells: $l = 2.0$, $h = 0.01$, $E_1/E_2 = 20$, $G_{12}/E_2 = 0.65$, $\nu_{12} = 0.25$.

Figures 4a and 4b present mode patterns for the CF cylindrical shells that have a symmetric four-layer sequence $[\alpha, -\alpha]_s$ and an antisymmetric sequence $[\alpha, -\alpha]_A$. The clamped edge is located at the lower end, as illustrated in the fifth mode in Fig. 4a. The patterns of the lowest five modes are presented for $\alpha = 25, 45,$ and 70 deg, and the corresponding frequencies λ are given.

It is seen in Fig. 4a that nodal lines are distorted because the principal material axes are skewed with angle-ply laminated layers. This tendency is not so distinct for antisymmetrically laminated shells in Fig. 4b, and their nodal patterns are similar to cross-ply laminated shells. For instance, this is seen clearly by comparing at the fifth modes of $\alpha = 45$ and 70 deg in Figs. 4a and 4b. In both ply patterns, however, the wave numbers for the corresponding mode sequence are the same and the transitions of nodal patterns are equally observed.

Summary and Conclusions

A unified approach has been developed for analyzing the free vibration of angle-ply laminated closed cylindrical shells. The Ritz method is used to derive the frequency equation, wherein newly developed displacement functions are introduced to automatically satisfy the prescribed geometric boundary conditions. The computer program code includes material constants, shell geometry, and edge conditions as input variables.

In the numerical examples, accuracy of the present solution is tested by convergence test and comparison with the results for cross-ply cases. The natural frequencies are obtained for a wide range of fiber angles, stacking sequence, and edge conditions. Mode shapes are also obtained for typical cases, and transition of the patterns is clearly observed.

The present method may be used as a design tool by structural engineers who are concerned with the dynamic behavior of composite shell structures. The present method is also applicable to optimization problems.

Acknowledgment

References

[1]Dong, S. B., "Free Vibration of Laminated Orthotropic Cylindrical Shells," *Journal of the Acoustical Society of America*, Vol. 44, No. 6, 1968, pp. 1628–1635.

[2]Dong, S. B., and Tso, F. K. W., "On a Laminated Orthotropic Shell Theory Including Transverse Shear Deformation," *Journal of Applied Mechanics*, Vol. 39, No. 4, 1972, pp. 1091–1097.

[3]Sun, C. T., and Whitney, J. M., "Axisymmetric Vibrations of Laminated Composite Cylindrical Shells," *Journal of the Acoustical Society of America*, Vol. 55, No. 6, 1974, pp. 1238–1246.

[4]Jones, R. M., and Morgan, H. S., "Buckling and Vibration of Cross-Ply Laminated Circular Cylindrical Shells," *AIAA Journal*, Vol. 13, No. 5, 1975, pp. 664–671.

[5]Uemura, M., "Vibration of Laminated Composite Cylindrical Shells," *Journal of the Japan Society for Aeronautical and Space Sciences*, Vol. 27, No. 307, 1979, pp. 382–388 (in Japanese).

[6]Sheinman, I., and Greif, S., "Dynamic Analysis of Laminated Shells of Revolution," *Journal of Composite Materials*, Vol. 18, No. 5, 1984, pp. 200–215.

[7]Reddy, J. N., "Exact Solutions of Moderately Thick Laminated Shells," *Journal of Engineering Mechanics ASCE*, Vol. 110, No. 5, 1984, pp. 794–809.

[8]Reddy, J. N., and Liu, C. F., "A Higher-Order Shear Deformation Theory of Laminated Elastic Shells," *International Journal of Engineering Science*, Vol. 23, No. 3, 1985, pp. 319–330.

[9]Reddy, J. N., and Khdeir, A. A., "Dynamic Response of Cross-Ply Laminated Shallow Shells According to a Refined Shear Deformation Theory," *Journal of the Acoustical Society of America*, Vol. 85, No. 6, 1989, pp. 2423–2431.

[10]Khdeir, A. A., and Reddy, J. N., "Influence of Edge Conditions on the Modal Characteristics of Cross-Ply Laminated Shells," *Computers and Structures*, Vol. 34, No. 6, 1990, pp. 817–826.

[11]Kobayashi, S., and Nagashima, T., "Vibration Characteristics of Laminated Graphite-Epoxy Circular Cylindrical Shells," *Journal of the Japan Society for Aeronautical and Space Sciences*, Vol. 34, No. 389, 1986, pp. 332–339 (in Japanese).

[12]Sheinman, I., and Weissman, S., "Coupling Between Symmetric and Antisymmetric Modes in Shells of Revolution," *Journal of Composite Materials*, Vol. 21, No. 11, 1987, pp. 988–1007.

[13]Sankaranarayanan, N., Chandrasekaran, K., and Ramaiyan, G., "Free Vibrations of Laminated Conical Shells of Variable Thickness," *Journal of Sound and Vibration*, Vol. 123, No. 2, 1988, pp. 357–371.

[14]Elishakoff, I., Cederbaum, G., and Librescu, L., "Response of Moderately Thick Laminated Cross-Ply Composite Shells Subjected to Random Excitation," *AIAA Journal*, Vol. 27, No. 7, 1989, pp. 975–981.